

General synchronization dynamics of coupled Van der Pol–Duffing oscillators

H.G. Enjieu Kadji^a, R. Yamapi^{b,*}

^aLaboratory of Nonlinear Modelling and Simulation in Engineering and Biological Physics, Faculty of Sciences, University of Yaounde I, P.O. Box 812, Yaounde, Cameroon

^bDepartment of Physics, Faculty of Sciences, University of Douala, P.O. Box 24157, Douala, Cameroon

Available online 17 April 2006

Abstract

This paper considers the general synchronization dynamics of coupled Van der Pol–Duffing oscillators. The linear and nonlinear stability analysis on the synchronization process is derived through the Whittaker method and the Floquet theory in addition to the multiple time scales method. A stability map displaying different dynamical states of the system is performed. Numerical simulation is carried out to support and to complement the accuracy of the analytical treatment.

© 2006 Elsevier B.V. All rights reserved.

PACS: 05.45.Gg; 05.45.Ac; 04.45.Pq

Keywords: Synchronization dynamics; Linear and nonlinear stability; Self-excited systems

1. Introduction

Synchronization is one of the fundamental phenomena in nature and it can be set up through nonlinear oscillators, both in their regular and chaotic states. Pecora and Carroll were the first to shed light on synchronization of chaotic oscillators by linking them with common signals [1]. Using the continuous feedback scheme of Pyragas [2], Kapitaniak also shows that it is possible to synchronize two chaotic oscillators [3]. Potential applications of synchronization in communication engineering (using chaos to mask the information bearing signals) [1,4–6], in physics (Josephson junctions arrays) [7], chemistry (discrete reaction–diffusion) [8] and in biology (circadian rhythms, heartbeat generation) [9] explain the great interest devoted to such topic by the scientific community.

In view of studying the phase synchronization of nonlinear oscillator in 1998, Leung in Ref. [10] considered the synchronization of two classical Van der Pol oscillators with various types of couplings including the continuous feedback difference coupling of Pyragas [2]. In particular, he showed that synchronization is possible for some appropriate ranges of the coupling strength and that the synchronization time has a critical

*Corresponding author. Tel.: +237 932 93 76; fax: +237 340 75 69.

E-mail addresses: henjieu@yahoo.com (H.G. Enjieu Kadji), ryamapi@yahoo.fr (R. Yamapi).

slowing down character near the boundaries of the synchronization domain. Woafu and Kraenkel considered recently in Ref. [11] the problem of stability and duration time of the synchronization process between two classical Van der Pol oscillators. They showed that the critical slowing down behavior of the synchronization time and the boundaries of the synchronization domain can be estimated, at least approximately by analytical investigations. They also extended the study of the synchronization process when the oscillators were in the chaotic states.

This paper extends the calculations of Ref. [11] by considering the problem of general synchronization dynamics of two Van der Pol–Duffing (VdPD) oscillators coupled through the continuous feedback scheme of Pyragas [2]. The Whittaker method [12], the Floquet theory [12,13] and the multiple time scales method [13] are used to derive the stability condition and the optimal coupling strength of the synchronization process.

The paper is organized as follows. In the next section, after the presentation of the model, we derive the limit cycle solutions and deals with the problem statement. The establishment of the variational equations is derived in Section 3. Linear stability analysis and the nonlinearity effects on the stability boundaries are also considered in Section 4. We presented in Section 5 analytical and numerical results. The last section is devoted to the conclusion.

2. The Van der Pol–Duffing oscillator

2.1. Dynamics of the Van der Pol–Duffing oscillator

The classical VdPD oscillator which appears in many physical problems is governed by the following nonlinear equation:

$$\ddot{x} - \mu(1 - x^2)\dot{x} + x + \alpha x^3 = 0, \quad (1)$$

where the overdot represents the derivative with respect to time, μ and α are two positive coefficients. It describes electrical circuits and has many applications in science, engineering and also displays a rich variety of nonlinear dynamical behaviors [14,15]. It generates the limit cycle which can be evaluated through the Lindsted's perturbation method [12,16]. It can be noticed that, the limit cycle is known to be a fairly strong attractor since it attracts all trajectories except the one initiated from the trivial fixed point $(x_0, \dot{x}_0) = (0, 0)$. For this purpose, to permit the amplitude and the frequency to interact, it is interesting to set $\tau = \omega t$, where ω is an unknown frequency. We assume that the periodic solution of (1) can be performed by the following approximation:

$$x(\tau) = x_0(\tau) + \mu x_1(\tau) + \mu^2 x_2(\tau) + \dots, \quad (2)$$

where $x_i(\tau)$ ($i = 0, 1, 2, \dots$) are periodic functions of τ of period 2π . Moreover, the frequency ω can be represented by an expansion having the form

$$\omega = \omega_0 + \mu\omega_1 + \mu^2\omega_2 + \dots, \quad (3)$$

where ω_i ($i = 0, 1, 2, 3, \dots$) are unknown constant at this level. Assuming that $\alpha = \mu\alpha_0$ before substituting both expressions (3) and (2) in Eq. (1) and equating the coefficients of μ^0 , μ^1 and μ^2 to zero, we obtain the following equations at different orders of μ :

order μ^0 :

$$\omega_0^2 \ddot{x}_0 + x_0 = 0, \quad (4)$$

order μ^1 :

$$\omega_0^2 \ddot{x}_1 + x_1 = -2\omega_0\omega_1 \ddot{x}_0 + \omega_0(1 - x_0^2)\dot{x}_0 - \alpha_0 x_0^3, \quad (5)$$

order μ^2 :

$$\begin{aligned} \omega_0^2 \ddot{x}_2 + x_2 = & -2\omega_0\omega_1 \ddot{x}_1 - (\omega_1^2 + 2\omega_0\omega_2)\ddot{x}_0 + \omega_0(1 - x_0^2)\dot{x}_1 \\ & + \omega_1(1 - x_0^2)\dot{x}_0 - 2\omega_0 x_0 \dot{x}_0 x_1 - 3\alpha_0 x_0^2 x_1. \end{aligned} \quad (6)$$

Making use of $x_i(\tau + 2\pi) = x_i(\tau)$ and $\dot{x}_i(0) = 0$ to determine the unknown quantities, we obtain after the resolution of Eq. (4) that

$$x_0 = A_0 \cos \tau, \quad \omega_0 = 1, \quad (7)$$

where A_0 is the limit cycle amplitude at this order. Considering the expressions given through Eq. (7), Eq. (5) leads to

$$\ddot{x}_1 + x_1 = \left(2\omega_1 A_0 - \frac{3}{4}\alpha_0 A_0^3\right) \cos \tau + \left(\frac{A_0^3}{4} - A_0\right) \sin \tau + \frac{A_0^3}{4} \sin 3\tau - \frac{A_0^3}{4} \alpha_0 \cos 3\tau. \quad (8)$$

The solvability condition of Eq. (8) gives rise to the following relations:

$$A_0 = 2, \quad \omega_1 = \frac{3}{2}\alpha_0. \quad (9)$$

With the initial condition $\dot{x}_1(0) = 0$, the general expression for a periodic solution of Eq. (8) is given by

$$x_1 = A_1 \cos \tau + \frac{3}{4} \sin \tau + \frac{\alpha_0}{4} \cos 3\tau - \frac{1}{4} \sin 3\tau. \quad (10)$$

One should note that the value of A_1 will be determined through the resolution of Eq. (6) which takes the following form when considering the solution x_1 :

$$\begin{aligned} \ddot{x}_2 + x_2 = & \left[4\omega_2 + (2\omega_1 - 9\alpha_0)A_1 + 2\omega_1^2 + \frac{1 - 3\alpha_0^2}{4}\right] \cos \tau + \left[2A_1 + \frac{3}{2}\omega_1 - \frac{5}{4}\alpha_0\right] \sin \tau \\ & + \left[\frac{9}{2}\omega_1\alpha_0 - \frac{3}{2} - \frac{3}{2}\alpha_0^2 - 3\alpha_0 A_1\right] \cos 3\tau \\ & + \left[3A_1 - \frac{5}{2}\omega_1\right] \sin 3\tau + \left[\frac{7 - 3\alpha_0^2}{4}\right] \cos 5\tau + 2\alpha_0 \sin 5\tau. \end{aligned} \quad (11)$$

Thus, the condition of secularity for the solution $x_2(\tau)$ yields to the following expressions:

$$A_1 = -\frac{1}{2}\alpha_0, \quad \omega_2 = -\frac{27}{16}\alpha_0^2 - \frac{1}{16}. \quad (12)$$

Therefore, the solution of Eq. (1) is approximated by

$$x(t) = A \cos \omega t + \frac{\alpha}{4} \cos 3\omega t + \mu \left(\frac{3}{4} \sin \omega t - \frac{1}{4} \sin 3\omega t \right) + O(\mu^2), \quad (13)$$

with

$$A = 2 - \frac{1}{2}\alpha, \quad \omega = 1 + \frac{3}{2}\alpha - \frac{27}{16}\alpha^2 - \frac{1}{16}\mu^2 + O(\mu^3). \quad (14)$$

2.2. Statement of the problem

The final state of the VdPD oscillator is a sinusoidal limit cycle for small values of the coefficient μ , developing into relaxation oscillations when μ becomes large. One particular characteristics in the VdPD model is that its phase depends on initial conditions. Therefore, if two VdPD oscillators are launched with different initial conditions, their trajectory will finally circulate on the same limit cycle, but with different phases φ_1 and φ_2 . The objective of the synchronization in this case is to phase-lock the oscillators (phase synchronization) so that $\varphi_1 - \varphi_2 = 0$.

As we have quoted in the introduction, one aim of this survey is to study the stability and derive the characteristics of the synchronization of two VdPD oscillators. The master system is described by the component x while the slave system has the corresponding component y . The enslavement is carried out by coupling the slave to the master through the following scheme:

$$\begin{aligned} \ddot{x} - \mu(1 - x^2)\dot{x} + x + \alpha x^3 &= 0, \\ \ddot{y} - \mu(1 - y^2)\dot{y} + y + \alpha y^3 &= -K(y - x)H(t - T_0), \end{aligned} \quad (15)$$

where K is the feedback coupling coefficient, t the time, T_0 the onset time of the synchronization process and $H(z)$ is the Heaviside function defined as

$$H(z) = \begin{cases} 0 & \text{for } z < 0, \\ 1 & \text{for } z \geq 0. \end{cases}$$

Practically, this type of unidirectional coupling between the master system and the slave system can be done through a linear resistor R_c and a buffer. The buffer acts as a signal-driving element that isolates the master system variable from the slave system variable, thereby providing a one-way coupling. In the absence of the buffer the system represents two identical VdPD oscillators coupled by a common resistor R_c , when both the master and slave systems will mutually affect each other.

3. Nonlinear variational equation

When the synchronization process is launched, the slave system changes its configuration. We must assume that the process is stable to avoid irreversible damages to the system. It is then particularly important to develop criteria that guarantee the asymptotic stability of the process. To measure the closeness between the master and the slave at each time, let us introduce a new variable

$$\varepsilon(t) = y(t) - x(t). \tag{16}$$

The stability of the process is thus examined by the boundedness of $\varepsilon(t)$ which obeys to the following equation:

$$\ddot{\varepsilon} - \mu(1 - x^2)\dot{\varepsilon} + (2\mu x\dot{x} + 3\alpha x^2 + 1 + K)\varepsilon + 2\mu x\varepsilon\dot{\varepsilon} + \mu\varepsilon^2\dot{\varepsilon} + (\mu\dot{x} + 3\alpha x)\varepsilon^2 + \alpha\varepsilon^3 = 0. \tag{17}$$

Saying that the process is stable here means that the synchronization is really effective. To achieve the synchronization process, we have to be sure that ε goes to zero as t increases or is less than a given precision. The behavior of ε depends on K and on the form of the master x . For small values of μ , the master time evolution is described by Eq. (13). Thus, the above variational Eq. (17) takes the form

$$\ddot{\varepsilon} + [2\lambda + F(\tau)]\dot{\varepsilon} + G(\tau)\varepsilon + Q(\tau)\varepsilon^2 + R(\tau)\varepsilon\dot{\varepsilon} + a_2\varepsilon^2 + a_3\varepsilon^3 = 0, \tag{18}$$

where

$$\tau = \omega t, \quad \lambda = \frac{\mu}{2\omega} \left(\frac{A^2}{2} - 1 + \frac{\mu^2}{4} + \frac{\alpha^2}{32} \right), \quad a_2 = \frac{\mu}{\omega^2}, \quad a_3 = \frac{\alpha}{\omega^2},$$

while the following quantities $F(\tau)$, $G(\tau)$, $Q(\tau)$, $R(\tau)$, g_0 , f_{is} , f_{ic} and g_{is} and g_{ic} ($i = 1, 2, 3$) are given in Appendix A.1.

From the expression of $G(\tau)$, we find that if

$$K < K_b(\alpha) = -\frac{3\alpha}{2} \left(A^2 + \frac{\mu^2}{2} + \frac{\alpha^2}{16} \right) - 1, \tag{19}$$

$\varepsilon(t)$ will grow indefinitely leading the slave to continuously drift away from its original limit cycle. In this case, the feedback coupling is dangerous since it continuously adds energy to the slave system. We show respectively in Figs. 1 and 2 the phase portraits of the master and the slave when $\alpha = 0.01$ and $\alpha = 0.05$ for several different values of the feedback coupling coefficient K chosen in the domain $K < K_b(\alpha)$. It is found that there is no synchronization between the master and the slave when K decreases from K_b to infinity since the deviation between the slave and the master becomes large or increases indefinitely. Since the analytical investigation of the variational equation (17) is very difficult due to its nature, we first consider the linear stability analysis before taking into account the nonlinearities effects in the analysis of the variational equation.

3.1. Linear stability analysis

We first suppose that the measure of the nearness ε of the slave to the master is very small, so that one can neglect both quadratic and cubic terms. Then in the linear regime, Eq. (17) is reduced to

$$\ddot{\varepsilon} + [2\lambda + F(\tau)]\dot{\varepsilon} + G(\tau)\varepsilon = 0. \tag{20}$$

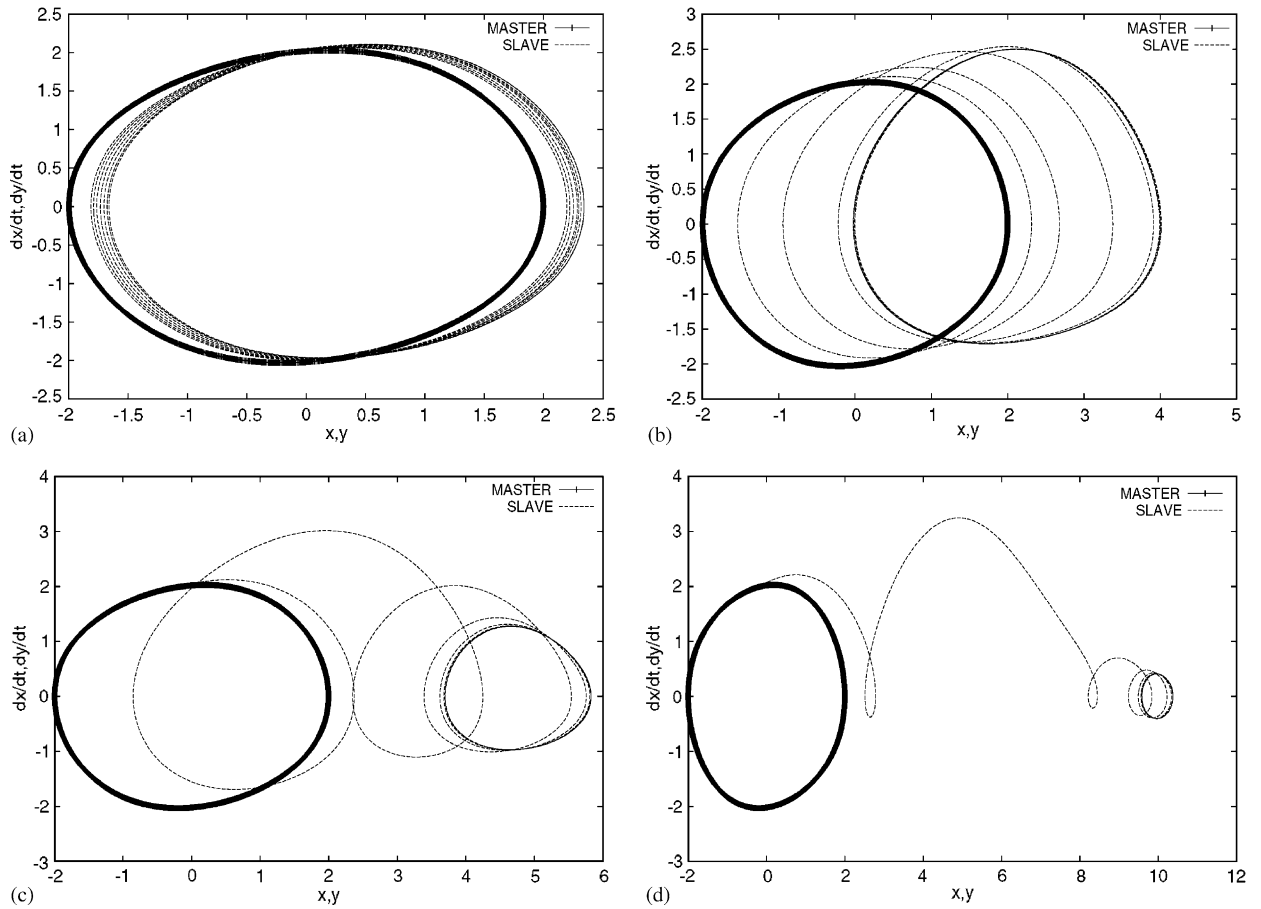


Fig. 1. Phase portrait of the master and the slave for several values of the coupling parameter K when $\alpha = 0.01$: (a) $K = -1.059$; (b) $K = -1.10$; (c) $K = -1.25$; (d) $K = -2.00$.

To examine the stability analysis of the synchronization process, let us transform Eq. (20) into the standard one by introducing a new variable η as follows

$$\varepsilon = \eta \exp(-\lambda\tau) \exp\left\{-\frac{1}{2} \int_0^\tau F(\tau') d\tau'\right\}. \quad (21)$$

This yields the following Hill equation:

$$\begin{aligned} \ddot{\eta} + (a_0 + 2a_{1c} \cos 2\tau + 2a_{1s} \sin 2\tau + 2a_{2c} \cos 4\tau \\ + 2a_{2s} \sin 4\tau + 2a_{3c} \cos 6\tau + 2a_{3s} \sin 6\tau + 2a_{4c} \cos 8\tau + 2a_{4s} \sin 8\tau \\ + 2a_{5c} \cos 10\tau + 2a_{5s} \sin 10\tau + 2a_{6c} \cos 12\tau + 2a_{6s} \sin 12\tau)\eta = 0, \end{aligned} \quad (22)$$

whose coefficients are given in Appendix A.2. Following the Floquet theory [12,13], the solution of Eq. (22) may be either stable or unstable and the stability boundaries of the synchronization process are to be found around the six main parametric resonances defined at $a_0 = n^2$ (with $n = 1, 2, 3, 4, 5, 6$). Therefore, using the Whittaker method [12], the solution of Eq. (22) in the n th unstable region may be assumed in the following form:

$$\eta = e^{\gamma\tau} \sin(n\tau - \zeta), \quad (23)$$

where γ is the characteristic exponent and ζ a parameter. Substituting Eq. (23) into Eq. (22) and equating the coefficients of $\cos n\tau$ and $\sin n\tau$ separately to zero, we obtain the following expression of the

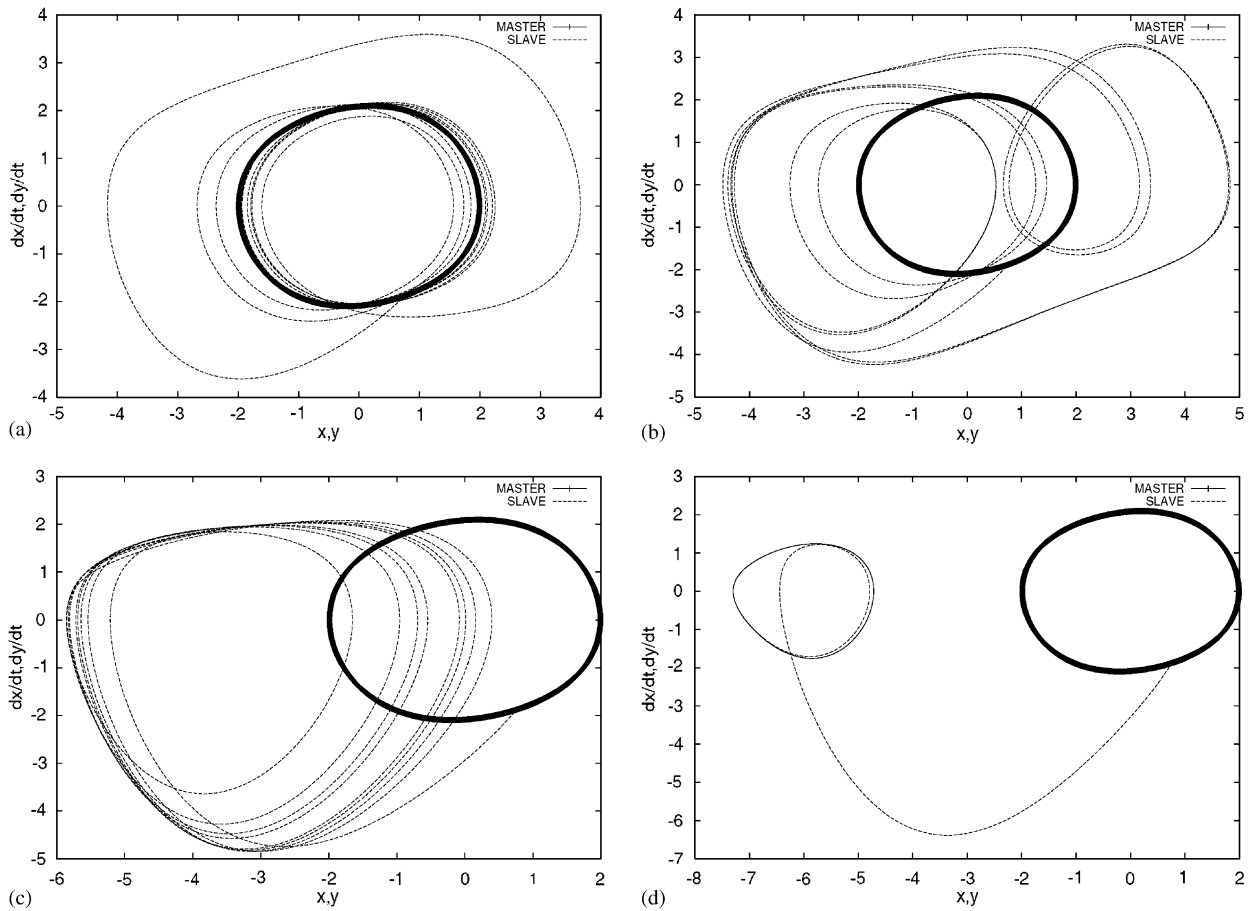


Fig. 2. Phase portrait of the master and the slave for several values of the coupling parameter K when $\alpha = 0.05$: (a) $K = -1.29$; (b) $K = -1.50$; (c) $K = -2.00$; (d) $K = -3.00$.

characteristic exponent:

$$\gamma^2 = -(a_0 + n^2) + \sqrt{4n^2a_0 + a_n^2}, \tag{24}$$

with $a_n^2 = a_{nc}^2 + a_{ns}^2$.

The synchronization process is achieved when ε goes to zero with increasing time, so that the real parts of $-\lambda \pm \gamma$ should be negative. Consequently, the synchronization process is stable under the condition

$$H^n = (a_0 - n^2)^2 + 2(a_0 + n^2)\lambda^2 + \lambda^4 - a_n^2 > 0, \quad n = 1, 2, 3, 4, 5, 6. \tag{25}$$

The above inequality will allow us to seek analytically the range of the coupling coefficient K where the process of synchronization is stable in the linear regime.

3.2. Effects of nonlinearities

After the stability of the synchronization process has been analyzed through the linear variational Eq. (20) in the previous section, we are going to tackle the variational equation in the general expression which contains cubic and quadratic nonlinearities. We aim to show the influence of nonlinearities on the stability domains obtain via the linear analysis. Thus, to search both effects of nonlinearities and parametric excitations, we use the method of multiple time scales [13]. Then, the solution of Eq. (18) can be

taken as follows

$$\varepsilon(\tau, \kappa) = \varepsilon_0(T_0, T_1) + \kappa\varepsilon_1(T_0, T_1) + \dots, \quad (26)$$

where $T_0 = \tau$, $T_1 = \kappa\tau$ and κ a small dimensionless parameter. Therefore, the variational Eq. (18) can be rewritten as

$$\begin{aligned} \ddot{\varepsilon} + g_0\varepsilon = & - [2\lambda + f_{1c} \cos 2\tau + f_{1s} \sin 2\tau + f_{2c} \cos 4\tau + f_{2s} \sin 4\tau]\dot{\varepsilon} \\ & - [g_{1c} \cos 2\tau + g_{1s} \sin 2\tau + g_{2c} \cos 4\tau + g_{2s} \sin 4\tau + g_{3c} \cos 6\tau + g_{3s} \sin 6\tau]\varepsilon \\ & - 2[q_{1c} \cos \tau + q_{1s} \sin \tau + q_{3c} \cos 3\tau + q_{3s} \sin 3\tau]\varepsilon^2 \\ & - 2[r_{1c} \cos \tau + r_{1s} \sin \tau + r_{3c} \cos 3\tau + r_{3s} \sin 3\tau]\varepsilon\dot{\varepsilon} - a_2\varepsilon^2\dot{\varepsilon} - a_3\varepsilon^3. \end{aligned} \quad (27)$$

Here, we just analyze the combined effects of the parametric excitation and the cubic nonlinearity. Then, we assume that

$$\lambda = \kappa\lambda, \quad f_{ic} = \kappa f_{ic}, \quad f_{is} = \kappa f_{is}, \quad g_{ic} = \kappa g_{ic}, \quad g_{is} = \kappa g_{is}, \quad a_2 = \kappa a_2,$$

$$a_3 = \kappa a_3, \quad q_{ic} = \kappa^2 q_{ic}, \quad q_{is} = \kappa^2 q_{is}, \quad r_{ic} = \kappa^2 r_{ic}, \quad r_{is} = \kappa^2 r_{is},$$

so that the effects of nonlinearities and the parametric excitation appear in the same order. Substituting Eq. (26) into Eq. (27) and equating the coefficients of κ^0 and κ^1 in both sides enable us to obtain

$$D_0^2\varepsilon_0 + \Omega_0^2\varepsilon_0 = 0, \quad (28)$$

$$\begin{aligned} D_0^2\varepsilon_1 + \Omega_0^2\varepsilon_1 = & - 2D_0D_1\varepsilon_0 - [2\lambda + f_{1c} \cos 2\tau + f_{1s} \sin 2\tau + f_{2c} \cos 4\tau \\ & + f_{2s} \sin 4\tau]D_0\varepsilon_0 - [g_{1c} \cos 2\tau + g_{1s} \sin 2\tau + g_{2c} \cos 4\tau \\ & + g_{2s} \sin 4\tau + g_{3c} \cos 6\tau + g_{3s} \sin 6\tau]\varepsilon_0 - a_2\varepsilon_0^2D_0\varepsilon_0 - a_3\varepsilon_0^3, \end{aligned} \quad (29)$$

where $\Omega = \sqrt{g_0}$, $D_0 = \partial/\partial T_0$ and $D_1 = \partial/\partial T_1$. The solution of Eq. (28) can be expressed as

$$\varepsilon_0(T_0, T_1) = A(T_1)\exp(j\Omega T_0) + \bar{A}(T_1)\exp(-j\Omega T_0), \quad (30)$$

where $j^2 = -1$. Taking into account the solution ε_0 , Eq. (29) now becomes

$$\begin{aligned} D_0^2\varepsilon_1 + \Omega^2\varepsilon_1 = & \{-2j\Omega A' - 2j\Omega\lambda A - 3a_3A^2\bar{A} - j\Omega a_2A^2\bar{A}\}\exp(j\Omega T_0) \\ & + \left\{\frac{1}{2}j\Omega f_{1c} + \frac{1}{2}\Omega f_{1s} - \frac{1}{2}\Omega g_{1c} + \frac{1}{2}j\Omega g_{1s}\right\}\bar{A}\exp[-j(\Omega - 2)T_0] \\ & + \left\{\frac{1}{2}j\Omega f_{2c} + \frac{1}{2}\Omega f_{2s} - \frac{1}{2}g_{2c} + \frac{1}{2}j\Omega g_{2s}\right\}\bar{A}\exp[-j(\Omega - 4)T_0] \\ & + \left\{\frac{1}{2}jg_{3s} - \frac{1}{2}g_{3c}\right\}\bar{A}\exp[-j(\Omega - 4)T_0] \\ & + \left\{-\frac{1}{2}j\Omega f_{1c} - \frac{1}{2}\Omega f_{1s} - \frac{1}{2}g_{1c} + \frac{1}{2}jg_{1s}\right\}A\exp[j(\Omega + 2)T_0] \\ & + \left\{-\frac{1}{2}j\Omega f_{2c} - \frac{1}{2}\Omega f_{2s} - \frac{1}{2}g_{2c} + \frac{1}{2}jg_{2s}\right\}A\exp[j(\Omega + 4)T_0] \\ & + \left\{\frac{1}{2}jg_{3s} - \frac{1}{2}g_{3c}\right\}A\exp[j(\Omega + 6)T_0] - \{j\Omega a_2 - a_3\}A^3\exp(3j\Omega T_0) + CC, \end{aligned} \quad (31)$$

where CC denotes the complex conjugate of the previous terms and the prime over $A(T_1)$ indicates a differentiation with respect to T_1 . We restrict our analysis in the case of the first parametric resonance (i.e., $g_0 \simeq 1$) and then perform the first approximation only. To express the nearness of g_0 to 1, let us introduce the detuning parameter σ which indicate the accuracy of the first parametric resonance as $\Omega + \kappa\sigma = 1$.

Consequently, the solvability condition of Eq. (31) is defined as

$$\begin{aligned}
 & -2j\Omega A' - 2j\Omega\lambda A - j\Omega a_2 A^2 \bar{A} - 3a_3 A^2 \bar{A} \\
 & + \left\{ \frac{1}{2}j\Omega f_{1c} + \frac{1}{2}jg_{1s} + \frac{1}{2}\Omega f_{1s} - \frac{1}{2}g_{1c} \right\} \bar{A} \exp(2i\sigma T_1) = 0.
 \end{aligned}
 \tag{32}$$

Taking $A(T_1) = \frac{1}{2}a(T_1) \exp[jb(T_1)]$ in Eq. (32) where $a(T_1)$ and $b(T_1)$ are respectively, the amplitude and the phase of the oscillations, we obtain the following set of first order differential equations after separating real and imaginary parts:

$$\begin{aligned}
 a' &= -\lambda a - \frac{a_2}{8}a^3 + \frac{1}{4\Omega}(\Omega f_{1c} + g_{1s})a \cos \Psi + \frac{1}{4\Omega}(\Omega f_{1s} - g_{1c})a \sin \Psi, \\
 \frac{1}{2}\Psi' &= \sigma - \frac{3a_3}{8\Omega}a^2 + \frac{1}{4\Omega}(\Omega f_{1s} - g_{1c}) \cos \Psi - \frac{1}{4\Omega}(\Omega f_{1c} + g_{1s}) \sin \Psi,
 \end{aligned}
 \tag{33}$$

where $\Psi = 2\sigma T_1 - 2b$. The steady motions appear when $a' = \Psi' = 0$ and we obtain the following algebraic equation:

$$(\theta^2 + \delta^2)a_s^4 + 2(\rho\theta + \zeta\delta)a_s^2 + \rho^2 + \zeta^2 - 1 = 0,
 \tag{34}$$

where

$$\begin{aligned}
 \theta &= \frac{\Omega a_2(\Omega f_{1s} - g_{1c}) - 3(\Omega f_{1c} + g_{1s})a_3}{2[(\Omega f_{1s} - g_{1c})^2 + (\Omega f_{1c} + g_{1s})^2]}, \\
 \delta &= \frac{2(\Omega f_{1c} + g_{1s})\theta + 3a_3}{2(\Omega f_{1s} - g_{1c})}, \\
 \rho &= \frac{4\Omega[\lambda(\Omega f_{1s} - g_{1c}) + \sigma(\Omega f_{1c} + g_{1s})]}{(\Omega f_{1s} - g_{1c})^2 + (\Omega f_{1c} + g_{1s})^2}, \\
 \zeta &= \frac{(\Omega f_{1c} + g_{1s})\rho - 4\Omega\sigma}{\Omega f_{1s} - g_{1c}}.
 \end{aligned}$$

In the exact principal parametric resonance ($\sigma = 0$), it comes from Eq. (34) the solutions

$$a_{s\pm}^2 = \frac{-\rho\theta - \delta\zeta \pm \sqrt{\Delta}}{\theta^2 + \delta^2},
 \tag{35}$$

with

$$\Delta = (\rho\theta + \delta\zeta)^2 - (\theta^2 + \delta^2)(\rho^2 + \zeta^2 - 1).$$

Consequently, we find that at the first approximation, the solution can be written as

$$\varepsilon = a_s \cos(\tau - \frac{1}{2}\Psi) + O(\kappa).
 \tag{36}$$

One should keep in mind that at the steady-state motion, the existence of amplitudes a_s depends straightforwardly to the value of the coupling coefficient K . When K varies, the frequency Ω is modified and a_s exist only if a_s^2 is positive. The stability of the steady-state motions of the solution $\varepsilon(\tau, \mu)$ can be determined by analyzing the nature of the steady-state solutions of Eqs. (33). That is why we let

$$\begin{aligned}
 a &= a_s + a_1, \\
 \Psi &= \Psi_s + \Psi_1,
 \end{aligned}
 \tag{37}$$

where a_s and Ψ_s are respectively the amplitude and the phase of the steady-state solutions. Keeping expressions (37) into Eqs. (33), expanding for small a_1 , Ψ_1 and taking linear quantities to a_1 and Ψ_1 lead us to

$$\begin{aligned}
 a_1' &= \Gamma a_1 + \Lambda \Psi_1, \\
 \Psi_1' &= \Xi a_1 + \Upsilon \Psi_1,
 \end{aligned}
 \tag{38}$$

where

$$\begin{aligned}\Gamma &= -\lambda - \frac{3}{8}a_2a_s^2 + \frac{(\Omega f_{1s} - g_{1c})}{4\Omega} \sin \Psi_s + \frac{(\Omega f_{1c} + g_{1s})}{4\Omega} \cos \Psi_s, \\ \Lambda &= \frac{(\Omega f_{1s} - g_{1c})}{4\Omega} \cos \Psi_s a_s - \frac{(\Omega f_{1c} + g_{1s})}{4\Omega} \sin \Psi_s a_s, \\ \Xi &= -\frac{3a_3}{2\Omega} a_s, \quad \Upsilon = -\frac{\Omega f_{1s} - g_{1c}}{2\Omega} \sin \Psi_s - \frac{\Omega f_{1c} + g_{1s}}{2\Omega} \cos \Psi_s, \\ \sin \Psi_s &= \rho + \theta a_s^2, \quad \cos \Psi_s = \zeta + \delta a_s^2.\end{aligned}$$

Thus, the stability of the process depends on the eigenvalues S of Eqs. (38) which are given through the following equation:

$$S^2 - (\Gamma + \Upsilon)S + \Gamma\Upsilon - \Lambda\Xi = 0. \quad (39)$$

The steady-state motions are then stable under the following conditions:

$$\begin{aligned}H_{nl}^1 &= -(\Gamma + \Upsilon) > 0, \\ H_{nl}^2 &= \Gamma\Upsilon - \Lambda\Xi > 0\end{aligned} \quad (40)$$

and unstable otherwise. At the exact internal resonance, the conditions (40) correspond to the domain of the coupling coefficient K in which $\varepsilon(t, \kappa)$ is stable when the time increases and therefore the stability condition for the process of synchronization in the nonlinear limit is defined. Now, we are going to use the both criteria (25) and (40) to seek respectively the range of the coupling parameter K where the process is linearly and nonlinearly stable.

4. Analytical and numerical results

The conditions (25) and (40) have been called to seek the range of the coupling parameter where the synchronization process is stable. It is important to note that for $n = 2, 3, 4, 5, 6$, the conditions (25) are satisfied for any value of K , and we only use this condition around the first main parametric resonance ($n = 1$). To identify different dynamical states which appears in the coupled VdPD oscillators, we varied the coefficient K to see if the conditions (25) and (40) are simultaneously verified or not. We find from these two conditions (25) and (40), that depending for the coupling coefficient K , there are some domains where the synchronization process could be stable or not. We fix $\mu = 0.1$ and used two values of α . For instance when $\alpha = 0.01$, the synchronization is unstable for $K \in]-\infty, -1.0597] \cup [-0.3130, 0[\cup]0, 0.260]$ while for $\alpha = 0.05$, the process is not achieved for $K \in]-\infty, -1.2929] \cup [-0.4550, 0[\cup]0, 0.1690]$. Saying here that the synchronization is unstable means that $\varepsilon(t)$ never goes to zero as the time is increased but has a bounded oscillatory behavior or goes to infinity. Three ranges of the coupling parameter are found. The first region is $K \in]-\infty, -1.0597]$ for $\alpha = 0.01$ and $K \in]-\infty, -1.2928]$ for $\alpha = 0.05$ where the synchronization process is unstable linearly and nonlinearly, called global unstable domain of the synchronization process. Generally in that first region, the amplitude of oscillations becomes very large and tend to infinity for certain values of the coupling parameter K (see Fig. 3a with $\alpha = 0.01$ and $K = -30$). Nevertheless according to α , the deviation $x - y$ between the master and the slave can be bounded by high-amplitude oscillations as shown in Fig. 3b for $\alpha = 0.05$ and $K = -30$. Such a behavior is the characteristic of global unstable phenomena of the synchronization process analyzed. In the second region, $K \in [-0.3130; 0[\cup]0; 0.260]$ for $\alpha = 0.01$ and $K \in]-0.4551, 0[\cup]0; 0.1690]$ for $\alpha = 0.05$, the synchronization is not achieved as we mentioned before since the deviation $x - y$ is bounded (see Fig. 4). Here, the amplitude of oscillations are very small compared to those observed in the global unstable. At the last region, $K \in]-1.0597, -0.3131[\cup]0.260, +\infty[$ for $\alpha = 0.01$ and $K \in]-1.2929, -0.4550[\cup]0.1690, +\infty[$ for $\alpha = 0.05$, the synchronization process is stable and defined what is called the global stability area. This means that the deviation between the master and the slave goes to zero as the time increases as we show in Fig. 5(a) for $\alpha = 0.01$ and in Fig. 5(b) for $\alpha = 0.05$.

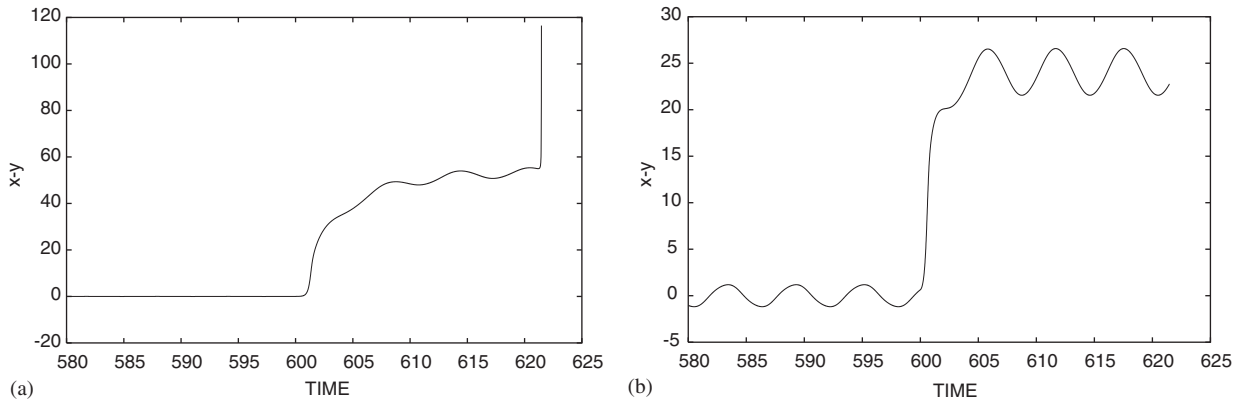


Fig. 3. Time history of the deviation $\varepsilon(t)$ displaying both linear and nonlinear unstable phenomena of the synchronization process: (a) $\alpha = 0.01$, $K = -30$; (b) $\alpha = 0.05$, $K = -30$.

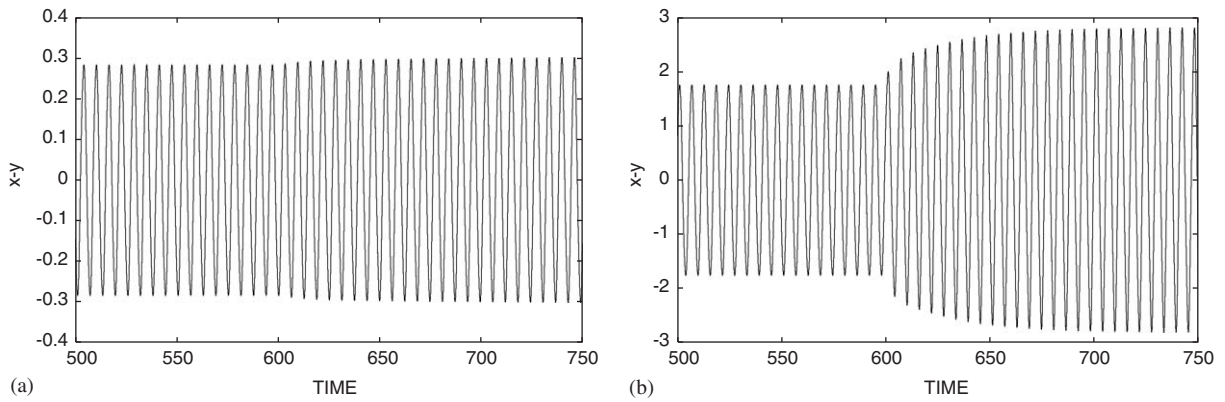


Fig. 4. Time history of the deviation $\varepsilon(t)$ displaying bounded oscillations in the process of synchronization: (a) $\alpha = 0.01$, $K = -0.04$; (b) $\alpha = 0.05$, $K = -0.35$.

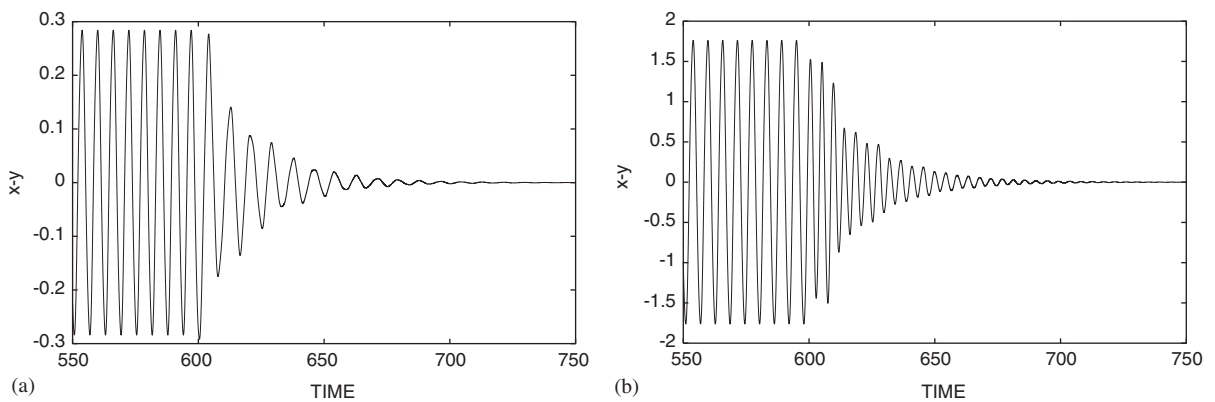


Fig. 5. Time history of the deviation $\varepsilon(t)$ displaying the stability of the synchronization process: (a) $\alpha = 0.01$, $K = -0.50$; (b) $\alpha = 0.05$, $K = 0.70$.

Numerical simulations have been used via the fourth-order Runge–Kutta algorithm with the time step $\Delta t = 10^{-2}$ in order to check the accuracy of our analytical investigation. Thus, both numerical and analytical results have led us to derive a stability chart in the plane (K, α) . Our results are reported in Fig. 6 and the coming results are observed.

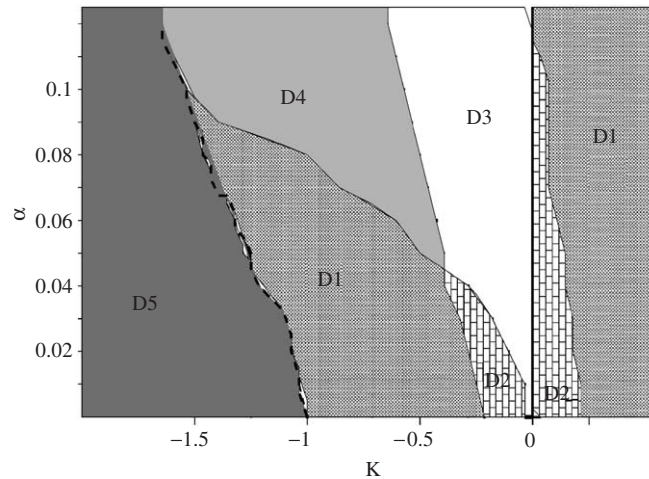


Fig. 6. Stability chart in the (K, α) plane.

Five different domains D_1, D_2, D_3, D_4, D_5 are distinguished. The first one (D_1) corresponds to the numerical and analytical (linear and nonlinear) stability domain, while D_2 is the region where the synchronization is stable numerically but analytically stable nonlinearly and unstable linearly. The closeness $\varepsilon(t)$ between the master and the slave in D_1 and D_2 tends to zero as it appears in Fig. 5, we remind that the configuration point (K, α) is in the global stable area. In the region D_3 , coexist analytically the linear instability, the nonlinear stability and the numerical instability. The deviation $x - y$ has a bounded oscillatory behavior as it appears in Fig. 4. We find that the region D_4 displays analytically both linear and nonlinear stabilities in addition to the numerical instability of the synchronization process. The last domain D_5 is both unstable analytically (linearly and nonlinearly) and numerically (global unstable area). It should be quoted that for some values of $K \in [-0.3130, 0] \cup [0, 0.260]$ (for instance, $K = -0.30; -0.20; 0.15$) when $\alpha = 0.01$, the synchronization process is numerically achieved while not predicted by the analytical investigations. But for $\alpha = 0.05$, there is a quite good agreement between both analytical and numerical results for all values of K . Therefore, it should be stressed that as the nonlinearity coefficient α increases, there is a good convergence between analytical and numerical results.

5. Conclusion

In this paper, we have investigated the general synchronization of two coupled VdPD oscillators. The analytical investigation of both linear and nonlinear stabilities is based on the Whittaker method and the Floquet theory, and also on the multiple time scales method. We have found that the amplitude of the oscillatory states is related to the coefficient of nonlinearity. The effects of such a coefficient on the stability boundaries of the synchronization process have also been found.

Appendix A

A.1. Appendix

The functions $F(\tau)$, $G(\tau)$, $R(\tau)$ and $R(\tau)$ are defined as

$$F(\tau) = f_{1c} \cos 2\tau + f_{1s} \sin 2\tau + f_{2c} \cos 4\tau + f_{2s} \sin 4\tau + f_{3c} \cos 6\tau + f_{3s} \sin 6\tau,$$

$$G(\tau) = g_0 + g_{1c} \cos 2\tau + g_{1s} \sin 2\tau + g_{2c} \cos 4\tau + g_{2s} \sin 4\tau + g_{3c} \cos 6\tau + g_{3s} \sin 6\tau,$$

$$Q(\tau) = 2q_{1c} \cos \tau + 2q_{1s} \sin \tau + 2q_{3c} \cos 3\tau + 2q_{3s} \sin 3\tau,$$

$$R(\tau) = 2r_{1c} \cos \tau + 2r_{1s} \sin \tau + 2r_{3c} \cos 3\tau + 2r_{3s} \sin 3\tau,$$

with

$$f_{1c} = \frac{\mu}{2\omega} \left(A^2 + \frac{\alpha A}{2} - \frac{15\mu^2}{16} \right), \quad f_{1s} = \frac{\mu^2}{2\omega} \left(A - \frac{3\alpha}{8} \right),$$

$$f_{2c} = \frac{\mu}{4\omega} \left(\alpha A + \frac{3\mu^2}{4} \right), \quad f_{2s} = \frac{\mu^2}{4\omega} \left(\frac{3\alpha}{4} - A \right),$$

$$f_{3c} = \frac{\mu}{\omega} \left(\frac{\alpha^2 - \mu^2}{32} \right), \quad f_{3s} = -\frac{\alpha\mu^2}{16\omega},$$

$$g_0 = \frac{1}{\omega^2} \left[1 + K + \frac{3\alpha}{2} \left(A^2 + \frac{\mu^2}{2} + \frac{\alpha^2}{16} \right) \right],$$

$$g_{1c} = \frac{3\alpha}{2\omega^2} \left(A + \frac{\alpha A}{2} - \frac{15\mu^2}{16} \right) + \frac{\mu^2}{\omega} \left(A - \frac{3\alpha}{8} \right),$$

$$g_{1s} = \frac{3\mu\alpha}{2\omega^2} \left(A - \frac{3\alpha}{8} \right) + \frac{\mu}{\omega} \left(-A^2 - 2\alpha A + \frac{15\mu^2}{16} \right),$$

$$g_{2c} = \frac{3\alpha}{4\omega^2} \left(\alpha A + \frac{3\mu^2}{4} \right) + \frac{\mu^2}{\omega} \left(-A + \frac{3\alpha}{4} \right),$$

$$g_{2s} = -\mu \left(\frac{7A + 3\mu^2}{4\omega} \right) + \frac{3\alpha\mu}{4\omega^2} \left(\frac{3\alpha}{4} - A \right),$$

$$g_{3c} = \frac{3\alpha(\alpha^2 - \mu^2)}{32\omega^2} + \frac{3\mu^2\alpha}{8\omega}, \quad g_{3s} = -\frac{3\alpha^2\mu}{16\omega^2} + \frac{3\mu(\mu^2 - \alpha^2)}{16\omega}.$$

A.2. Appendix

The quantities a_0 , a_{ns} and a_{nc} are defined as

$$a_0 = g_0 - \lambda^2 - \frac{1}{8}(f_{1c}^2 + f_{1s}^2 + f_{2c}^2 + f_{2s}^2 + f_{3c}^2 + f_{3s}^2),$$

$$a_{1c} = \frac{1}{2}g_{1c} + \frac{1}{2}f_{1s} - \frac{1}{8}(4\lambda f_{1c} + f_{1c}f_{2c} + f_{1s}f_{2s} + f_{2c}f_{3c} + f_{2s}f_{3s}),$$

$$a_{1s} = \frac{1}{2}g_{1s} - \frac{1}{2}f_{1c} - \frac{1}{8}(4\lambda f_{1s} + f_{1c}f_{2s} + f_{2c}f_{3s} - f_{2s}f_{3c}),$$

$$a_{2c} = \frac{1}{2}g_{2c} + f_{2s} - \frac{1}{8}(\frac{1}{2}f_{1c}^2 - \frac{1}{2}f_{1s} + 4\lambda f_{2c} + f_{1c}f_{3c} + f_{1s}f_{3s}),$$

$$a_{2s} = \frac{1}{2}g_{2s} - f_{2c} - \frac{1}{8}(4\lambda f_{2s} + f_{1c}f_{1s} + f_{1c}f_{3s} - f_{1s}f_{3c}),$$

$$a_{3c} = \frac{1}{2}g_{3c} + \frac{3}{2}f_{3s} - \frac{1}{8}(4\lambda f_{3c} + f_{1c}f_{2c} - f_{1s}f_{2s}),$$

$$a_{3s} = \frac{1}{2}g_{3s} - \frac{3}{2}f_{3c} - \frac{1}{8}(4\lambda f_{3s} + f_{1c}f_{2s} - f_{1s}f_{2c}),$$

$$a_{4c} = -\frac{1}{8}(\frac{1}{2}f_{2c}^2 - \frac{1}{2}f_{2s}^2 + f_{1c}f_{3c} - f_{1s}f_{3s}),$$

$$a_{4s} = -\frac{1}{8}(f_{1c}f_{3s} - f_{1s}f_{2c} + f_{1s}f_{3c} + f_{2s}f_{2c}),$$

$$a_{5c} = -\frac{1}{8}(f_{2c}f_{3c} - f_{2s}f_{3s}), \quad a_{5s} = -\frac{1}{8}(f_{2c}f_{3s} + f_{2s}f_{3c}),$$

$$a_{6c} = \frac{f_{3s}^2 - f_{3c}^2}{16}, \quad a_{6s} = -\frac{1}{8}f_{3c}f_{3s}.$$

References

- [1] L.M. Pecora, T.L. Carroll, *Phys. Rev. Lett.* 64 (1990) 821.
- [2] K. Pyragas, *Phys. Lett. A* 170 (1992) 421.
- [3] T. Kapitaniak, *Phys. Rev. E* 50 (1994) 1642.
- [4] A.V. Oppenheim, G.V. Wornell, S.H. Isabelle, K. Cuomo, Signal processing in the context of chaotic signals, *Proceedings of International Conference on Acoustic, Speech and Signal Processing*, vol. i4, IEEE, New York, pp. 117–120.
- [5] L.J. Kocarev, K.S. Halle, K. Eckert, U. Parlitz, L.O. Chua, *Int. J. Bifur. Chaos* 2 (1992) 709.
- [6] G. Perez, H.A. Cerdeira, *Phys. Rev. Lett.* 74 (1995) 1970.
- [7] K. Wiesenfeld, P. Hadley, *Phys. Rev. Lett.* 62 (1989).
- [8] Y. Kuramoto, *Chemical Oscillations, Waves and Turbulence*, Springer, Berlin, 1980.
- [9] A.T. Winfree, *The Geometry of Biological Time*, Springer, New York, 1980.
- [10] H.K. Leung, *Phys. Rev. E* 58 (1998) 5704.
- [11] P. Wofo, R.A. Kraenkel, *Phys. Rev. E* 65 (2002) 036225.
- [12] C. Hayashi, *Nonlinear Oscillations in Physical Systems*, Mc-Graw Hill, New York, 1964.
- [13] A.H. Nayfeh, D.T. Mook, *Nonlinear Oscillations*, Wiley-Interscience, New York, 1979.
- [14] W. Szemplińska-Stupnicka, J. Rudowski, *Phys. Lett. A* 192 (1994) 201.
- [15] A. Venkatesan, M. Lakshamanan, *Phys. Rev. E* 56 (1997) 6321.
- [16] P. Hagedorn, *Nonlinear Oscillations*, Clarendon Press, Oxford, 1989.